

Developmental changes in left and right ventricular diastolic filling patterns in mice

Yu-Qing Zhou,^{1,3,6} F. Stuart Foster,^{2,5,6} Robert Parkes,¹ and S. Lee Adamson^{1,3,4}

¹Samuel Lunenfeld Research Institute, Mount Sinai Hospital; ²Sunnybrook & Women's College Health Sciences Centre; Departments of ³Physiology, ⁴Obstetrics/Gynecology, and ⁵Medical Biophysics, University of Toronto; and ⁶Mouse Imaging Centre, Hospital for Sick Children, Toronto, Ontario, Canada M5G 1X5

Submitted 29 April 2003; accepted in final form 30 May 2003

Zhou, Yu-Qing, F. Stuart Foster, Robert Parkes, and S. Lee Adamson. Developmental changes in left and right ventricular diastolic filling patterns in mice. *Am J Physiol Heart Circ Physiol* 285: H1563–H1575, 2003. First published June 12, 2003; 10.1152/ajpheart.00384.2003.—Developmental changes in left and right ventricular diastolic filling patterns were determined noninvasively in isoflurane-anesthetized outbred ICR mice. Blood velocities in the mitral and tricuspid orifices were recorded in 16 embryos at *days 14.5* (E14.5) and *17.5* of gestation (E17.5) using an ultrasound biomicroscope and also serially in three groups of postnatal mice aged 1–7 days ($n = 23$), 1–4 wk ($n = 18$), and 4–12 wk ($n = 27$) using 20-MHz pulsed Doppler. Postnatal body weight increased rapidly to 8 wk. Heart rate increased rapidly from ~ 180 beats/min at E14.5 to ~ 380 beats/min at 1 wk after birth and then more gradually to plateau at ~ 450 beats/min after 4 wk. Ventricular filling was quantified using the ratio of peak velocity of early ventricular filling due to active relaxation (E wave) to that of the late ventricular filling caused by atrial contraction (A wave) (peak E/A ratio) and the ratio of the peak E velocity to total time-velocity integral of E and A waves (peak E/total TVI ratio). Both ventricles had similar diastolic filling patterns in embryos (peak E/A ratio of 0.28 ± 0.02 for mitral flow and 0.27 ± 0.02 for tricuspid flow at E14.5). After birth, mitral peak E/A increased to >1 between the third and fifth day, continued to increase to 2.25 ± 0.25 at ~ 3 wk, and then remained stable. The tricuspid peak E/A ratio increased much less but stabilized at the same age (increased to 0.79 ± 0.03 at 3 wk). The peak E/total TVI ratio showed similar left-right differences and changes with development. Age-related changes were largely due to increases in peak E velocity. The results suggest that diastolic function matures ~ 3 wk postnatally, presumably in association with maturation of ventricular recoil and relaxation mechanisms.

mitral orifice; tricuspid orifice; pulsed Doppler; cardiac hemodynamics; ultrasound biomicroscope; isoflurane

VENTRICULAR DIASTOLIC FUNCTION, particularly that of the left ventricle, has been extensively studied in humans using pulsed Doppler echocardiography. This method is used to noninvasively monitor the pattern of the ventricular filling waves produced by active ventricular relaxation during early diastole (E wave) and by atrial contraction during late diastole (A wave). The

peak velocity ratio of the E and A waves (peak E/A ratio) is most often used to quantify ventricular diastolic function. The evaluation of the ventricular diastolic filling pattern is important because diastolic dysfunction contributes substantially to the production of symptoms in various cardiac disorders including congestive heart failure, coronary artery disease, hypertension, dilated and hypertrophic cardiomyopathy, and amyloid heart disease, and it often precedes the onset of systolic dysfunction (23, 26, 27). In human fetal cardiomyopathy, ventricular diastolic dysfunction, relative to systolic dysfunction, is associated with a significantly higher risk of perinatal mortality (32).

Genetically engineered mice have been used to model human cardiac diseases. As in humans, diastolic dysfunction occurs in association with cardiac hypertrophy in various transgenic or mutant mouse models (3, 4). With the use of Doppler methods, abnormal diastolic function has also been observed in phospholamban-deficient mice (16) and hyperthyroid mice (38). In senescent mice, the mitral peak E/A ratio is significantly decreased (38), suggesting that, as in humans, diastolic dysfunction develops during aging. However, most studies reporting ventricular diastolic filling patterns in mice are limited to the adult left ventricle (16, 33, 40) or to the embryonic heart without differentiating the left and right ventricles (12, 24, 41). Little information on diastolic ventricular function is available for either the mouse neonate or juvenile or for the right ventricle throughout development. This information is important for the critical evaluation of mice as potential models of human cardiac disease.

In the present study, left and right ventricular diastolic filling waveforms were examined during late gestational development in mice using a newly developed ultrasound biomicroscope (9, 10, 43, 51). The study began on *day 14.5* of gestation (E14.5), when the interventricular septum fully separates the ventricular inflow tracts of the embryonic heart (19, 36), and measurements were made by placing the Doppler sample volume discretely within the left or right ventricular inflow tracts with the guidance of a high-resolution ultrasound image. We also examined the left and right

Address for reprint requests and other correspondence: S. L. Adamson, Samuel Lunenfeld Research Institute, Mount Sinai Hospital, Rm. 138P, 600 Univ. Ave., Toronto, Ontario, Canada M5G 1X5 (E-mail: adamson@mshri.on.ca).

The costs of publication of this article were defrayed in part by the payment of page charges. The article must therefore be hereby marked "advertisement" in accordance with 18 U.S.C. Section 1734 solely to indicate this fact.

ventricular diastolic filling waveforms throughout postnatal development from birth to the young adult. Measurements were made using a 20-MHz transcutaneous pulsed Doppler system in the absence of a two-dimensional ultrasound image, a method previously validated in studies of left ventricular filling in adult mice (15, 38, 39).

MATERIALS AND METHODS

The study protocol was approved by the Mount Sinai Hospital Animal Care Committee, and the study was conducted in accordance with the guidelines of the Canadian Council on Animal Care.

Prenatal study. Pregnant mice (ICR, wild type, Harlan Sprague Dawley; Indianapolis, IN) were studied on E14.5 and *day 17.5* of gestation (E17.5) (where 18.5 days is full term), and a total of 16 embryos (1–3 embryos from each of 8 pregnant mice) were observed at each time point. *Day 0.5* of gestation was defined as noon on the day a vaginal plug was found after overnight mating. Mice were anesthetized by face mask with ~1.5% isoflurane (the minimum required to suppress spontaneous body movements). Body temperature was monitored via a rectal thermometer and maintained at 36–38°C using a heating pad and lamp, and heart rate was also monitored via transcutaneous electrodes (Indus Instruments; Houston, TX). All hair was removed from the abdomen by shaving, followed by a chemical hair remover (Nair, Carter-Horner; Mississauga, Ontario, Canada). To provide a coupling medium for the transducer, a warmed thick ultrasound gel was placed around the margin, and a thinner gel was put in the central area. The recording was started after ~1–2 min passed for the mouse to stabilize.

An ultrasound biomicroscope (VS40, VisualSonics; Toronto, Ontario, Canada) with the transducer frequency set at 40 MHz (for lateral and axial resolutions of 68 and 38 μm , respectively) was used to image embryonic cardiac structures. The pulsed Doppler operating frequency was set at 20 MHz to measure blood flow velocities. The Doppler sample volume was 104 μm (lateral) by 257 μm (axial). The pulse repetition frequency was set at 25 kHz to achieve a maximum measurable velocity of ~50 cm/s (10, 51). With these settings, we sampled flow spectra separately from mitral and tricuspid orifices of the embryonic heart on E14.5 and E17.5 (Fig. 1).

One to three embryos with an orientation that permitted a transverse section of the embryonic chest and a good overall view of the atrioventricular inflow channels were selected in each pregnant mouse (Fig. 1). The left and right ventricles were identified. Visible flow streams generated by echogenic embryonic blood (37) facilitated accurate placement of the Doppler sample volume within the mitral and tricuspid orifices, and the intercept angle was measured and used when calculating blood flow velocity. Doppler flow spectra were recorded for at least five consecutive cardiac cycles and transferred to a Doppler signal processing workstation (DSPW, Indus Instruments) for postanalysis. The whole procedure (from the onset of anesthesia to the end of data collection) took ~20–30 min. The mouse was returned to the cage after waking up in ~1–3 min.

Postnatal study. Three groups of wild-type ICR mice were studied serially in overlapping age ranges. We used multiple groups to limit repeated experiments on individuals, thereby reducing possible developmental effects. In the neonatal group, 23 neonates from 2 litters were studied every other day from 1 to 7 days after birth. In the preweaning group, 18 mice from 2 litters were studied weekly from 1 to 4 wk after birth. The gender was not identified in neonatal and

preweaning groups. In the postweaning group, 27 mice (12 males and 15 females from 2 litters) were followed every 4 wk from 4 to 12 wk of age.

Postnatal mice were anesthetized as described above for pregnant mice. Heart rate and body temperature were monitored as above in the postweaning group. Heat and anesthetic settings were the same in the neonatal and preweaning groups, but heart rate and body temperature were not monitored. Any hair on the precordial region was cleanly shaved, and the region was covered with prewarmed ultrasound gel.

A 20-MHz transcutaneous pulsed Doppler instrument (Valpey-Fisher; Hopkinton, MA) was used to sample the flow spectrum from mitral and tricuspid orifices. The size of the transducer was ~2 mm in diameter, and the sample volume was ~0.5 \times 0.5 \times 0.5 mm³. The ultrasound biomicroscope was not used for velocity measurements because postnatal blood velocities exceeded the biomicroscope's upper limit. However, the biomicroscope was used to measure the range depth required to reach the atrioventricular orifices from a point on the chest near the apex of the heart (~3.5 mm for neonates and 5–7 mm for adults). The optimal transducer orientation during flow sampling was ~45° to the body surface for postnatal mice at all ages.

The Doppler transducer was placed on the skin near the apical region of the heart and then pointed rostrally to the animal's posterior and right side to sample the mitral flow waveform first. Typically, two consecutive peaks (e.g., E and A waves) were observed in each cardiac cycle. For tricuspid flow, the transducer was slowly angled further toward the animal's right until the mitral flow disappeared and then further to the right until another waveform with two consecutive peaks appeared (Fig. 2). The tricuspid flow spectrum had a lower amplitude than the mitral flow spectrum and exhibited greater and opposite variation with respiration. During inspiration, tricuspid flow velocity increased (for both E and A waves, but to a variable extent for each), whereas mitral flow velocity slightly decreased (both E and A wave) (Figs. 2 and 3, *B* and *D*), as observed in humans (26). Systolic outflow and diastolic inflow waves were often detected at the same Doppler sample volume location in the left ventricle but not in the right ventricle (Figs. 1–3). We adjusted the direction and sampling depth of the transducer to obtain flow spectra with the highest possible amplitude. As suggested by human studies (26), the smallest flow area is at the level of the mitral and tricuspid valve tips and therefore the velocity is the highest there. Velocity at this site is believed to best reflect the pressure gradient between the atrium and ventricle. No angle correction was made because it was assumed that the intercept angle between the ultrasound beam and flow direction was close to zero, so correction was not required. Doppler flow spectra for at least 10 consecutive cardiac cycles were recorded and then transferred to the DSPW and saved for postanalysis. The procedure from the onset of anesthesia to the end of data collection took ~5–10 min for the neonatal and preweaning groups and <15 min for the postweaning group. The mouse was then returned to its cage after waking up in ~1–2 min.

The specific shape of the left and right ventricular diastolic filling waveforms were confirmed in two mice at 12 wk of age by two-dimensional image-guided Doppler sampling using an Acuson Sequoia C256 with the transducer frequency at 13 MHz (Fig. 3) and also in six neonates at 1–9 days after birth by image-guided Doppler sampling using new ultrasound biomicroscope prototype software, which permitted velocity measurement up to ~80 cm/s (data not shown).

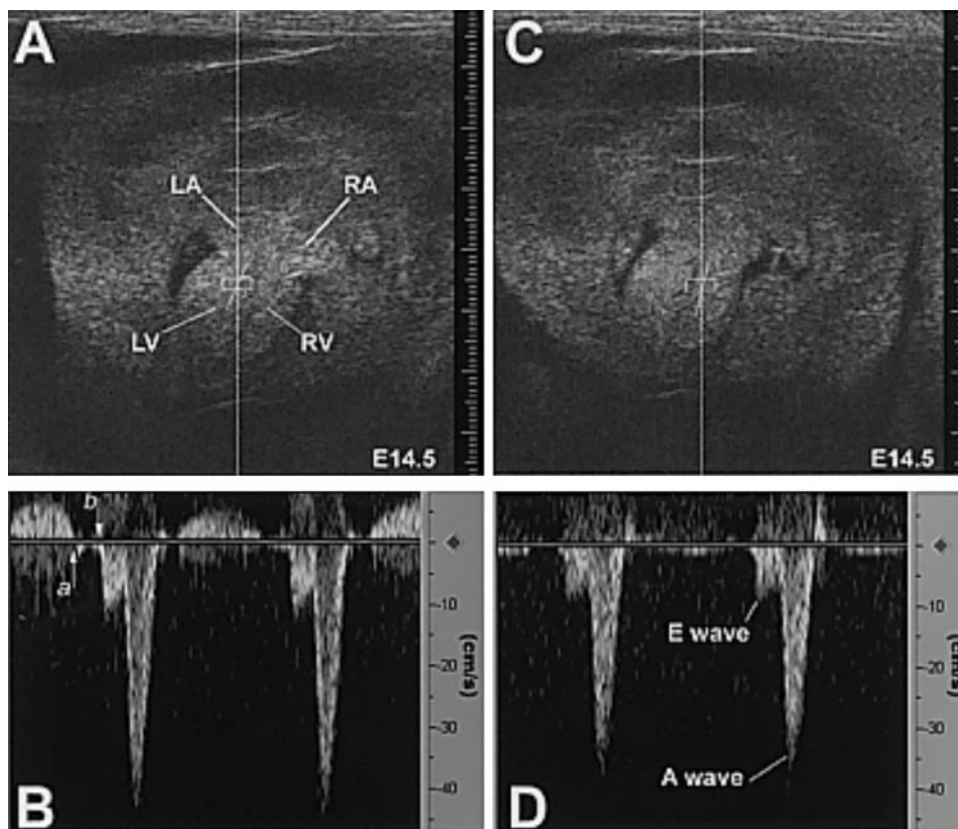


Fig. 1. Image-guided Doppler flow measurement in a mouse embryo heart at 14.5 days of gestation (E14.5) using the ultrasound biomicroscope. *A*: transverse view of the heart showing the left ventricular (LV) and right ventricular (RV) inflow tracts. Blood flowing into the ventricles was clearly visible because of the echogenic properties of embryonic blood, and flow direction was easily evaluated for the angle correction of Doppler flow velocity. The Doppler sample volume (white box) was located in the mitral orifice to sample the flow velocity. LA and RA, left and right atrium, respectively. *B*: Doppler spectrum obtained from the mitral orifice. The biphasic waveforms in the downward direction are the diastolic inflow spectra. In most Doppler recordings from the mitral valve, the outflow spectra was also visible, as in this example. The monophasic waveforms in the upward direction were caused by the Doppler sample volume including at least a portion of the adjacent LV outflow tract. This waveform was used to measure the LV isovolumic relaxation time [IVRT; i.e., the time interval from the end of outflow (arrow *a*) to the start of mitral inflow (arrow *b*)]. *C*: transverse image of the heart with the Doppler sample volume (white box) located in the tricuspid orifice. *D*: Doppler spectrum obtained from the tricuspid orifice. In *A* and *C*, the smallest division of the scale bar is 100 μm . In *B* and *D*, the ordinate shows blood velocity (in cm/s). E wave, early diastolic filling wave caused by ventricular relaxation; A wave, late diastolic filling wave caused by atrial contraction.

To evaluate the effect of anesthesia on the ventricular diastolic filling pattern, the mitral and tricuspid flows were recorded in 10 mice at 1 wk of age without anesthesia (at this age, mice were small enough to be held still) and compared with results from the neonatal group at the seventh day after birth obtained under anesthesia. In addition, in 10 mice at 2 wk postnatal age, after the mitral and tricuspid flow spectra were recorded under anesthesia as described above, the isoflurane vaporizer was turned off and the mouse was moved away from the mask. Continuous alternate recordings of mitral and tricuspid flow spectra were made until the mouse awoke (in 1–2 min), and recording became impossible due to the movement of the mouse. The data obtained at arousal were compared with those during anesthesia for each mouse.

Data analysis. Doppler waveforms were quantitatively analyzed using a DSPW and related software (Indus Instruments). The following parameters were measured and calculated: 1) R-R interval and heart rate; 2) the peak velocity of the E wave (peak E); 3) the peak velocity of the A wave (peak

A); 4) the ratio of peak E to peak A velocities (peak E/A ratio); 5) the time-velocity integral (or area) under the E and A waves (total TVI); and 6) the ratio of peak E velocity to the total TVI (peak E/total TVI ratio), which is considered a load-independent index of ventricular diastolic function according to human studies (17, 25, 29). The E and A waves were usually at least partially merged probably due to the high heart rate in mice, so it was impossible to define the real ending point of the E wave. For this reason, the time durations and areas (or TVIs) of the individual E wave and A wave and the related ratios were not determined. The left ventricular isovolumic relaxation time (IVRT) was measured when the diastolic inflow and systolic outflow waveforms were available in the same Doppler recording (Figs. 1–3). Left ventricular IVRT is the time interval between the end of the left ventricular outflow and the start of mitral inflow (24). To eliminate the effect of heart rate on this temporal parameter, the left ventricular IVRT was normalized to the R-R interval and expressed as a percentage of the cardiac cycle (%IVRT). Each parameter in the mouse embryo was aver-

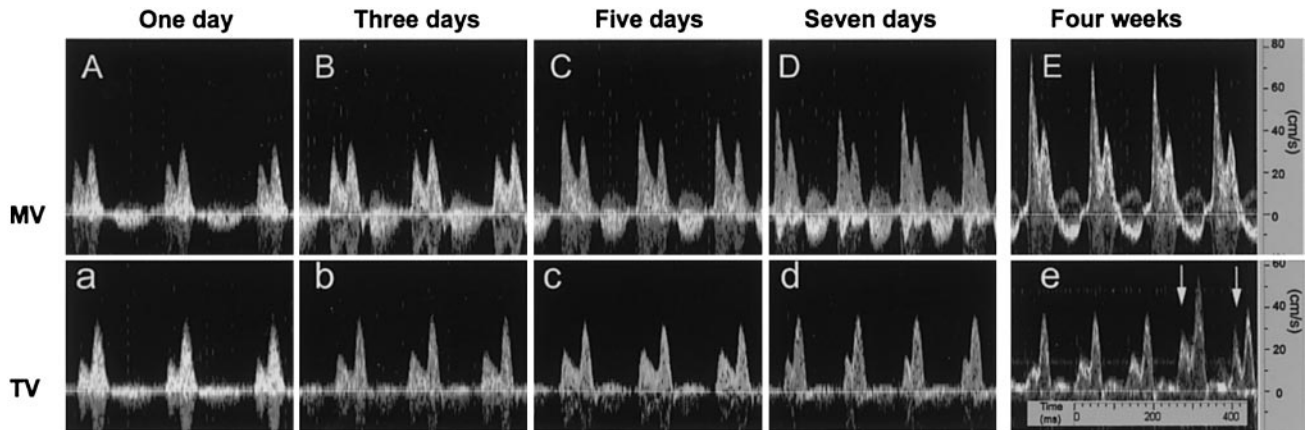


Fig. 2. Typical Doppler flow spectra obtained from the mitral orifice (A–E) and from the tricuspid orifice (a–e) in mouse neonates on the first, third, fifth, and seventh day after birth and in a mouse at weaning age (4 wk old). Arrows in *e* mark tricuspid waves acquired near the end of inspiration. Note the changes in waveform shape and amplitude. Time and velocity scales for all Doppler flow spectra are the same. MV, mitral valvular orifice; TV, tricuspid valvular orifice.

aged over five cardiac cycles. Each parameter in postnatal mice was averaged over 10 consecutive cardiac cycles to minimize the effect of variations caused by respiration.

Variability of tricuspid blood velocity measurements. In contrast with the available data for mitral flow (15, 38, 39), little data have been reported concerning the measurement of tricuspid flow in mice. Therefore, we evaluated interobserver variability in tricuspid flow measurement by comparing the results obtained by 2 independent operators within 1 session from 10 adult mice. For intersession variability, the tricuspid flow spectra from the same 10 mice were recorded twice by the same observer with a time interval of 1 wk. We chose the heart rate, peak E/A ratio, total TVI, and peak E/total TVI ratio for the evaluation of variability, because those parameters are most commonly used to quantify the ventricular diastolic filling pattern. Interobserver variability within one session and intersession variability with the same

observer were expressed as the percent discrepancy between two measurements (i.e., the absolute value of the difference between the two measurements divided by the mean of the two, expressed as a percentage).

Developmental changes in ventricular morphology. The morphology of the left and right ventricles changes during development and would be anticipated to affect ventricular filling patterns. The gross morphology of the right and left ventricles was observed in mouse embryos at E14.5 and E17.5, neonates at 1 day after birth, and in adults at 8 wk postnatal age. At E14.5 and E17.5, one pregnant mouse was euthanized while anesthetized with isoflurane, and two embryos were obtained. Two neonates and two adult mice were similarly euthanized, and the hearts were removed. Embryos and isolated postnatal hearts were fixed in 10% formalin for 24 h. Embryonic hearts were then removed under a microscope. Embryonic, neonatal, and adult hearts were embedded

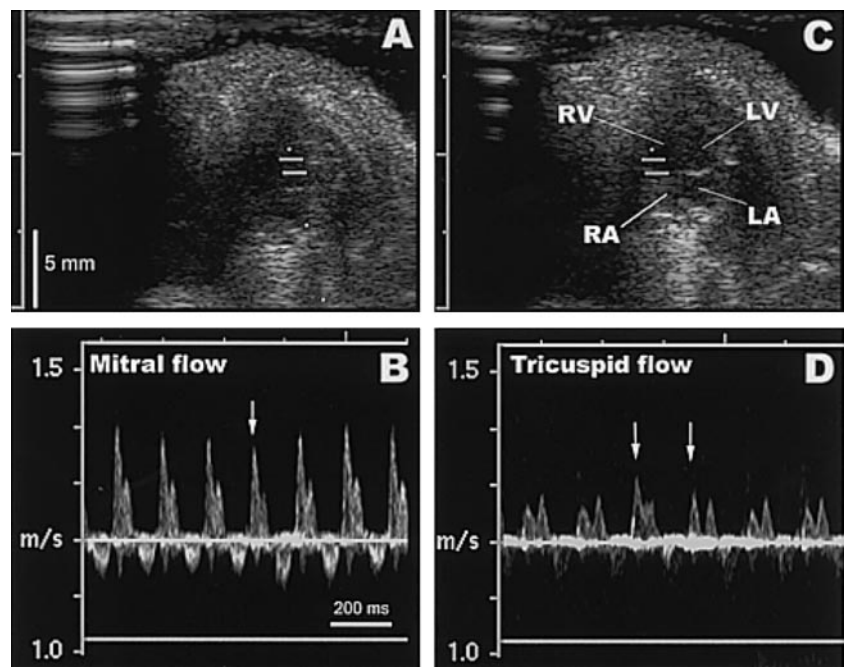


Fig. 3. Two-dimensional image guided pulsed Doppler flow sampling from the mitral and tricuspid orifices in an adult mouse using a clinical ultrasound system (Acuson Sequoia C256). A: apical four-chamber view of the heart with Doppler sample volume located in the mitral orifice (as indicated by =). B: Doppler flow spectrum obtained from the mitral orifice. C: apical four-chamber view of the heart with Doppler sample volume located in the tricuspid orifice (as indicated by =). D: Doppler flow spectrum obtained from the tricuspid orifice. Arrows in B and D mark waveforms acquired near the end of inspiration. Note that inspiration decreases inflow velocities in the mitral orifice but increases those in the tricuspid orifice.

in paraffin, 10- μ m serial sections were obtained, and slides were prepared and stained with hematoxylin and eosin. The slides from the middle portion between the cardiac base and apex were compared between age groups.

Statistical analysis. All results are presented as means \pm SE. Unpaired *t*-tests were used in the comparison of 1) mouse embryos at E14.5 versus E17.5, 2) anesthetized versus unanesthetized groups of 1-wk-old mice, and 3) male versus female mice at both 8 and 12 wk. A paired *t*-test was used to compare a group of 2-wk-old anesthetized mice before and after waking up. To observe the developmental change with advancing age, the measurements from every first session in each of embryonic, neonatal, preweaning, and postweaning groups were compared with each other. In all comparisons among the four age groups of mice, differences in SDs between groups made it necessary to use mixed linear models (45), with heterogeneous variances. For parameters with both mitral and tricuspid measurements, the correlation between the two orifices was modeled in the covariance matrix as well. Pairwise significance tests were carried out for each parameter, with *P* values adjusted for multiple comparisons using the simulated distribution of the maximum absolute value of a multivariate *t* random vector (7).

RESULTS

In the prenatal study, each pregnant mouse had \sim 10 embryos, and it was easy to find one to three embryos with optimal orientation for Doppler recording. Recordings from all studied embryos were included in the analysis. In the postnatal study, some mice were excluded from the analysis at several time points. Reasons included the complete fusion of E and A waves caused by high heart rate (in some adults of the postweaning group), death (neonatal group at the seventh day), or poor quality of the Doppler waveform. The numbers of included measurements at different time points are presented in Table 1.

There was a rapid postnatal increase in body weight from birth to 8 wk, followed by a more gradual increase to 12 wk of age (Fig. 4A). Heart rate significantly and rapidly increased during embryonic and neonatal development (E14.5 to 7 days postnatally) and then increased more gradually with advancing age into adulthood (Table 2 and Fig. 4B).

As Fig. 4C shows, in the embryo and early neonate, total TVIs in the mitral and tricuspid orifices were similar. Afterward, the total TVI of mitral flow increased with age to \sim 3 wk after birth, but that of

tricuspid flow did not increase throughout postnatal development (Table 2 and Fig. 4C).

Ventricular diastolic filling patterns. Table 2 summarizes the developmental changes in left and right ventricular diastolic filling patterns by comparing the first time point in each of the four age groups. The peak E velocity, peak E/A ratio, and peak E/total TVI ratio in the mitral and tricuspid orifices all significantly increased with age from E14.5 to 4 wk after birth. These variables of mitral and tricuspid orifices did not significantly differ before birth, whereas after birth the values from the mitral orifice were significantly greater than those from the tricuspid orifice. In contrast, peak A velocity did not change significantly with age in either orifice.

In mouse embryos, the lateral dimension (\sim 100 μ m) of the Doppler sample volume was much less than the width of the mitral and tricuspid orifices (300–350 μ m at E14.5 and 450–500 μ m at E17.5), so separate inflow waveforms could be readily obtained. Embryonic left and right ventricles had similar diastolic filling patterns (Fig. 1), with peak E/A ratios of <0.5 (Fig. 5A). From E14.5 to E17.5, there was a significant increase in heart rate ($P < 0.0001$; Fig. 4B), and approximately parallel increases for both ventricles in peak E velocity ($P < 0.0001$), peak A velocity (mitral: $P = 0.004$ and tricuspid: $P = 0.0002$), peak E/A ratio ($P < 0.0001$), and peak E/total TVI ratio ($P < 0.0001$) were observed (Fig. 5 and 6).

In neonatal mice, the ventricular diastolic flow pattern in the mitral orifice changed markedly in the first wk after birth (Fig. 2). At the time of birth, the peak E/A ratio was <1 for both ventricles (Fig. 5A). However, between the third and fifth day after birth, the mitral peak E/A ratio started to reverse, from <1 to >1 , and then continued to increase, mainly due to an increase in peak E velocity (Fig. 6A). After \sim 3 wk, the peak E/A ratio became relatively stable and remained at \sim 2 into adulthood (Fig. 5A). In the tricuspid orifice, peak E velocity showed a slight increase with age but was always lower than peak A velocity (Fig. 6B). The peak E/A ratio therefore remained <1 throughout the studied age range (Fig. 5A). In general, both mitral and tricuspid peak A velocities stayed relatively stable throughout the observed postnatal age range, although small fluctuations were observed (Fig. 6). The peak

Table 1. Numbers of studied mice and included measurements at different time points throughout development

| | Fetal Group | | Neonatal Group | | | | Preweaning Group | | | | Postweaning Group | | |
|----------------------------|-------------|-------|----------------|--------|--------|--------|------------------|------|------|------|-------------------|------|-------|
| | E14.5 | E17.5 | 1 day | 3 days | 5 days | 7 days | 1 wk | 2 wk | 3 wk | 4 wk | 4 wk | 8 wk | 12 wk |
| Number of studied mice | 16 | 16 | 23 | 23 | 23 | 19 | 18 | 18 | 18 | 18 | 27 | 27 | 27 |
| Number of measurements | 16 | 16 | 21 | 22 | 22 | 19 | 18 | 17 | 17 | 18 | 26 | 22 | 24 |
| Number of measured LV IVRT | 15 | 13 | 14 | 21 | 22 | 19 | 17 | 16 | 16 | 18 | 26 | 21 | 24 |

E14.5 and E17.5 represent the *day 14.5* and *day 17.5* of gestation, respectively. Neonatal group time periods represent the first, third, fifth, and seventh days after birth, respectively. Preweaning group and postweaning group time periods represent 1, 2, 3, 4, 8, and 12 wk of age, respectively. The number of measurements includes those for all parameters except for left ventricular (LV) isovolumic relaxation time (IVRT).

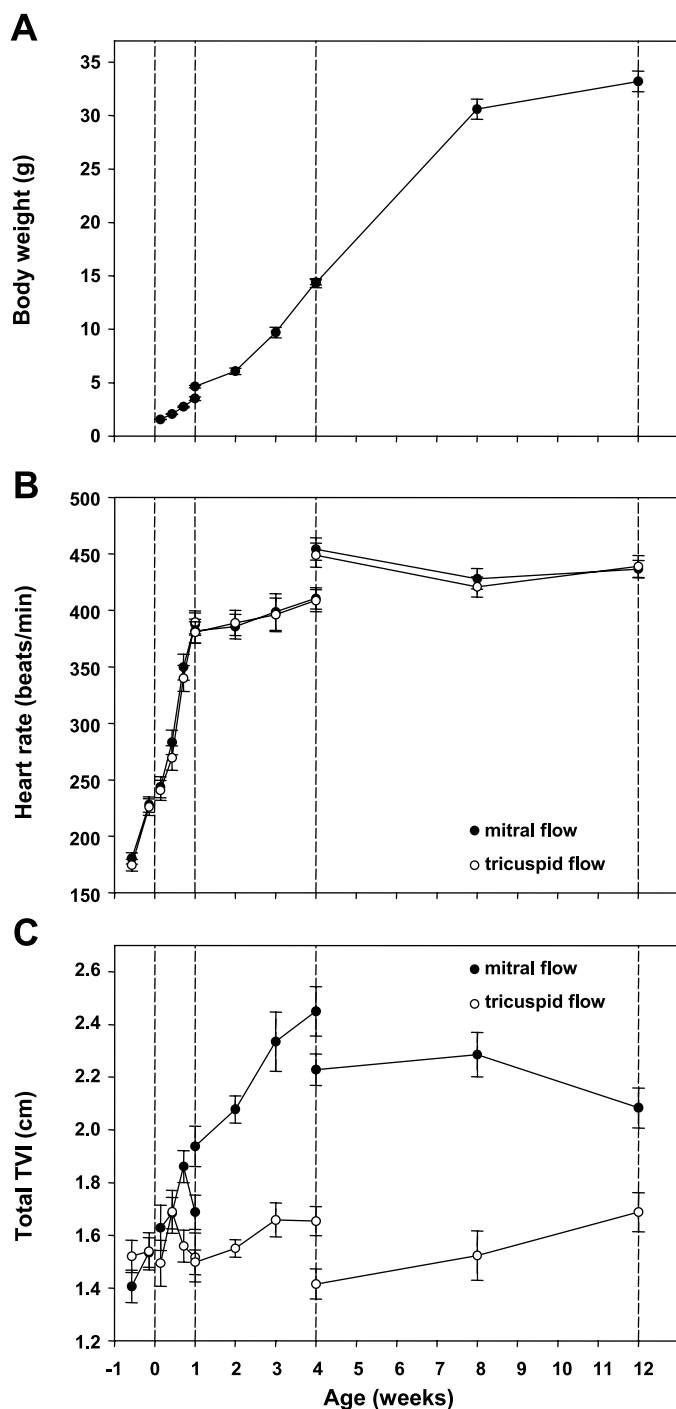


Fig. 4. Changes of mouse body weight (A), heart rate (B; in beats/min), and total time-velocity integrals (total TVI) of mitral and tricuspid flow (C) with development. The abscissa represent age (in wk), where zero denotes the time of birth. No significant difference was found between the heart rate derived from mitral versus tricuspid flow in B. In C, a significant difference ($P < 0.05$) was found between the total TVI of mitral flow and that of tricuspid flow at all time points except for those before birth and at days 1, 3, and 7 after birth. The vertical dashed lines divide data obtained from each of the four age groups.

E/total TVI significantly increased for both ventricles postnatally but to a much lesser extent in the right ventricle than in the left ventricle (Fig. 5B). From 1 day after birth to adulthood, the peak E/A ratio and peak

E/total TVI ratio were always significantly greater in the left ventricle than the right ventricle (Fig. 5, A and B, and Table 2).

Left ventricular IVRT gradually and significantly decreased from 47.4 ± 2.4 ms at E14.5 to 13.1 ± 0.03 ms at 4 wk after birth (Table 2) and then showed little further change with age (data not shown). %IVRT did not change significantly from $14.3 \pm 0.6\%$ at E14.5 to 1 wk after birth, but then decreased significantly between 1 and 4 wk after birth (to $9.8 \pm 0.2\%$), and remained consistent between 4 and 12 wk postnatal age (Table 2 and Fig. 5C). Doppler spectra collected for peak E and A velocity measurements were not always suitable for IVRT measurements, so the number of included measurements for IVRT at each time point were slightly less than for velocity measurements (Table 1).

In the postweaning group, the parameters from male and female subsets of mice were compared at 8 and 12 wk, and significant differences found only in the body weight and total TVI of mitral flow (Table 3).

Ventricular gross morphology at different ages. Figure 7 shows histological sections of the heart in the short-axis plane near the middle of the ventricles from embryos at E14.5 and E17.5, a neonate at 1 day, and an adult at 8 wk after birth. In adults, the left ventricular chamber is round, and its wall is morphologically dominant. In contrast, in the embryo at E14.5, both ventricular chambers were similar in shape and size, and their walls were of similar thickness. Left ventricle dominance appeared to emerge by 1 day after birth (Fig. 7).

Effect of anesthesia on the ventricular diastolic filling patterns. In 1-wk-old mice, ventricular diastolic filling patterns studied without anesthesia were similar to those studied under anesthesia (Table 4). There was no significant difference between the two groups in the peak E/A ratio, which is the most commonly used variable reflecting the diastolic filling pattern. Somewhat higher heart rates, peak E and A velocities, and total TVIs were observed in mice without anesthesia, which may be due to the stress of restraint (Table 4). In 2-wk-old mice, no significant differences were observed in parameters measured from mitral and tricuspid flow waveforms during anesthesia and at arousal except for a slight increase of the peak E/total TVI ratio in mitral flow (Table 5).

Reproducibility of measurements from tricuspid flow waveforms. The interobserver variability within sessions was $<7\%$ and the intersession variability was $<13\%$ for measurements of heart rate, peak E/A ratio, TVI, and peak E/total TVI ratio from the tricuspid flow waveform (Table 6).

DISCUSSION

The present study is the first to report the developmental changes of both left and right ventricular diastolic filling patterns in mice from embryonic to adult periods. The peak E/A ratio and peak E/total TVI ratio progressively increased and left ventricular %IVRT

Table 2. Comparison of left and right ventricular diastolic inflow parameters of mice at four different ages of development

| | Fetal Group at E14.5 | Neonatal Group at 1 Day | Prewaning Group at 1 Wk | Postweaning Group at 4 Wk |
|---|--------------------------|---------------------------|---------------------------|---------------------------|
| Number of measurements | 16 | 21 | 18 | 26 |
| Body weight, g | | 1.57 ± 0.02 ^A | 4.64 ± 0.11 ^B | 14.32 ± 0.41 ^C |
| Mitral flow | | | | |
| Heart rate, beats/min | 180 ± 5 ^A | 244 ± 9 ^B | 382 ± 11 ^C | 454 ± 10 ^D |
| Peak E, cm/s | 9.8 ± 0.6 ^A | 23.7 ± 1.3 ^B | 48.6 ± 2.3 ^C | 73.4 ± 1.7 ^D |
| Peak A, cm/s | 34.4 ± 1.3 ^A | 31.4 ± 1.6 ^A | 35.9 ± 1.4 ^A | 35.3 ± 1.6 ^A |
| Peak E/A ratio | 0.28 ± 0.02 ^A | 0.76 ± 0.02 ^B | 1.36 ± 0.03 ^C | 2.20 ± 0.10 ^D |
| Total TVI, cm | 1.4 ± 0.1 ^A | 1.6 ± 0.1 ^B | 1.9 ± 0.1 ^C | 2.2 ± 0.1 ^D |
| Peak E/total TVI ratio, s ⁻¹ | 7.0 ± 0.3 ^A | 14.7 ± 0.5 ^B | 25.1 ± 0.6 ^C | 33.2 ± 0.7 ^D |
| Tricuspid flow | | | | |
| Heart rate, beats/min | 174 ± 5 ^a | 241 ± 9 ^b | 381 ± 9 ^c | 449 ± 11 ^d |
| Peak E, cm/s | 8.9 ± 0.6 ^a | 15.6 ± 1.0 ^{b*} | 23.2 ± 0.9 ^{c*} | 28.2 ± 1.1 ^{d*} |
| Peak A, cm/s | 33.4 ± 0.9 ^a | 32.3 ± 1.1 ^a | 36.2 ± 1.0 ^a | 35.1 ± 1.6 ^a |
| Peak E/A ratio | 0.27 ± 0.02 ^a | 0.49 ± 0.03 ^{b*} | 0.65 ± 0.03 ^{c*} | 0.82 ± 0.03 ^{d*} |
| Total TVI, cm | 1.5 ± 0.1 ^a | 1.5 ± 0.1 ^a | 1.5 ± 0.1 ^{a*} | 1.4 ± 0.1 ^{a*} |
| Peak E/total TVI ratio, s ⁻¹ | 5.9 ± 0.3 ^a | 10.8 ± 0.6 ^{b*} | 15.6 ± 0.5 ^{c*} | 20.0 ± 0.4 ^{d*} |
| Number of measurements | 15 | 14 | 17 | 26 |
| LV IVRT, ms | 47.4 ± 2.4 ^A | 33.1 ± 2.1 ^B | 21.3 ± 0.7 ^C | 13.1 ± 0.3 ^D |
| LV %IVRT | 14.3 ± 0.6 ^A | 13.9 ± 0.5 ^A | 13.4 ± 0.3 ^A | 9.8 ± 0.2 ^B |

Values are means ± SE. Peak E, peak velocity of the early ventricular filling wave (E wave); peak A, peak velocity of the late ventricular filling wave due to atrial contraction (A wave); peak E/A ratio: the ratio of peak E to peak A; total TVI; the time-velocity integral (or total area) under E and A waves; peak E/total TVI ratio, the ratio of peak E velocity to total TVI; LV %IVRT: LV IVRT normalized to R-R interval and expressed as a percentage. Along each row, the same superscript letter means no significant difference among the values of the same parameter, whereas a different superscript letter indicates a significant difference ($P < 0.05$) among the values of the same parameter. Along each column, * indicates a significant difference ($P < 0.05$) compared with the corresponding value of mitral flow waveform at the same age.

progressively decreased during late gestation to reach mature levels at ~3 wk postnatally, indicating that rapid functional maturation of the heart occurred over this developmental interval. Whereas left and right ventricular diastolic filling patterns were similar in the embryo, they diverged during the first ~3 wk after birth. During this interval, there was a large increase in peak E velocity, whereas peak A wave velocity showed little change. The increase in peak E was more marked in the mitral orifice than the tricuspid orifice. Peak E/A and peak E/total TVI ratios showed similar left-right differences and changes with development. The results indicate that diastolic function matures ~3 wk postnatally, presumably in association with maturation of ventricular recoil and relaxation mechanisms.

Developmental changes in ventricular diastolic filling patterns. In the mouse embryo, the diastolic function of both ventricles significantly improved during prenatal development from E14.5 to E17.5, as indicated by the increase in peak E velocity (from 10 to 18 cm/s), peak A velocity (from 33 to 38 cm/s), and peak E/A ratio (from 0.25 to 0.4). These results are similar to prior studies over the same age range in mice but in which the left and right ventricular inflow tracts were not differentiated and/or were both contained within the relatively large Doppler sample volume of the clinical ultrasound systems (peak E velocity increased from 5–10 to ~13 cm/s, peak A velocity was ~33 cm/s, and peak E/A ratio increased from 0.1–0.3 to ~0.4) (12, 41). The peak E/A ratio of the embryonic heart in late gestation in the mouse (from 0.25 to 0.4) was lower than that of human embryos in late gestation, where the peak E/A ratio increases from ~0.60 at midgestation to ~0.85 at late gestation for both left and right

ventricles (29, 34). Thus our data suggest that, as in human embryos in late gestation, both ventricles in the mouse embryo display similar ventricular diastolic function and both show similar functional changes with gestational age. In mice, the peak E/A ratio is lower at birth than in humans, suggesting that diastolic function is less mature at birth in mice.

In postnatal mice, the mitral peak E/A ratio increased rapidly in the first 3 wk after birth and reached relatively high values of ~2.0–2.5 in the adult period. The mitral peak E/A ratio became >1 between 3 and 5 days after birth. In contrast, in humans, the mitral peak E/A ratio is >1 from the first day after birth (17, 47). The tricuspid peak E/A ratio also significantly increased during development in mice to reach ~0.8 in adulthood but, although it changed with a time course similar to that of the mitral peak E/A ratio, increments in peak E were much smaller and the peak E/A ratio remained <1 into adulthood. Comparatively, in humans, the tricuspid peak E/A ratio becomes >1 at ~6 mo of age (5). In human young adults, the mitral and tricuspid peak E/A ratios are similar, with a value of ~2 for both ventricles (18). This contrasts with mice, where mitral and tricuspid peak E/A ratios differ in young adults (8 wk), being ~2 and 0.7, respectively.

In the present study, developmental changes in E/A ratios were primarily due to the approximately sevenfold increase in mitral peak E (from ~10 to 70 cm/s) and approximately threefold increase in tricuspid peak E (from ~10 to 30 cm/s), whereas peak A velocity was similar between ventricles and relatively constant throughout development (~35 cm/s). In humans, over a similar developmental period (fetus to young adult), mitral peak E increases 2.7-fold (from ~30 to 80 cm/s)

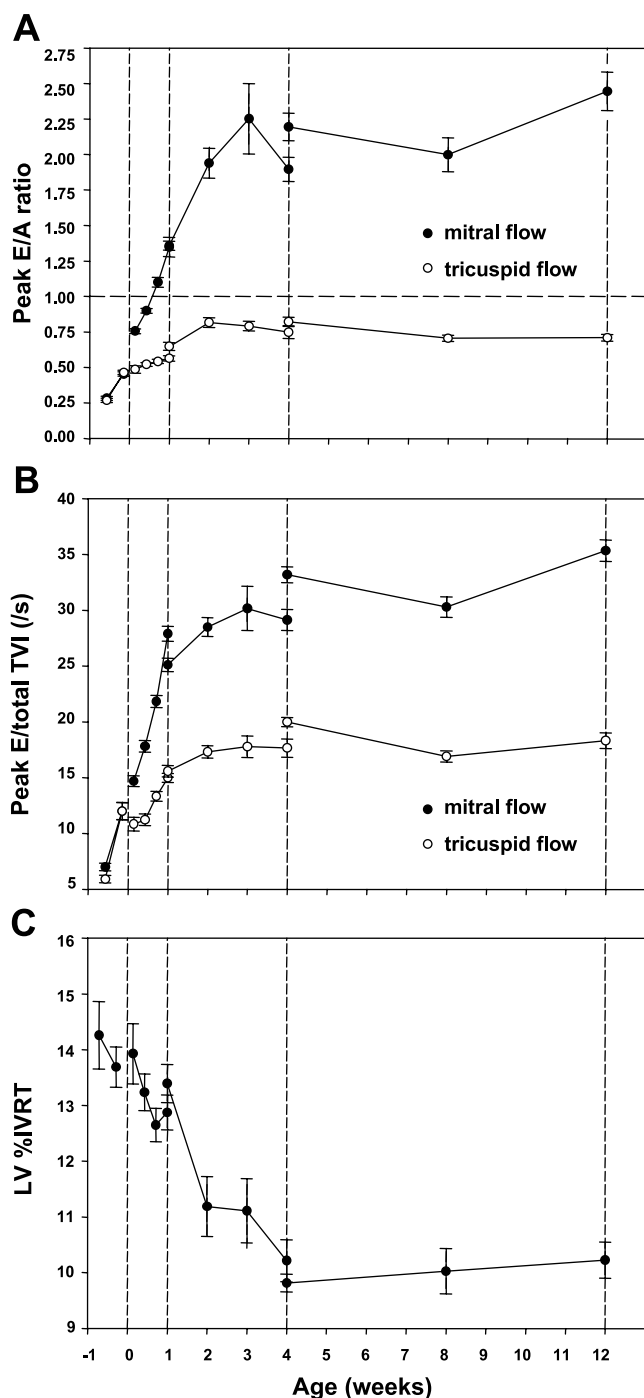


Fig. 5. Developmental changes of the ratio of peak E to peak A velocities (peak E/A ratio; A) and peak E velocity to total TVI ratio (peak E/total TVI ratio; B) for both mitral and tricuspid orifices and the LV IVRT expressed as a percentage of the cardiac cycle length (%IVRT) (C). The abscissa represent age (in wk), where zero denotes the time of birth. Significant differences ($P < 0.05$) were found in the peak E/A ratio and peak E/total TVI ratio between the mitral and tricuspid values at all time points except for the embryonic period. The vertical dashed lines divide data obtained from each of the four age groups.

and tricuspid peak E increases ~ 1.4 -fold (from ~ 35 to 50 cm/s), whereas peak A velocity remains relatively constant in the mitral orifice (~ 40 cm/s) but decreases in the tricuspid orifice (from ~ 45 to <30 cm/s) (34, 34,

47, 50). Thus, in both species, there is a maturational increase in peak E velocity that is greater in the left ventricle than in the right ventricle, and peak A velocity is relatively constant with development in the left ventricle. The species differ more markedly in the right ventricle. In mice, tricuspid peak E velocity is much lower than that in humans throughout development and peak A velocity does not decrease with development as in humans.

The period of rapidly increasing peak E velocity (which ended at ~ 3 wk) did not coincide with the period of rapidly increasing heart rate (which ended at ~ 1 wk) or body weight (which ended at ~ 8 wk). Nor did it coincide with the period of rapid growth of the mouse heart, which ends at ~ 8 – 10 wk of age (2, 34). The early ventricular filling wave (E wave) is mainly generated by active myocardial relaxation and by ventricular recoil. Thus the developmental increase in peak E velocity may be related to the developmental increase in the capacity of the sarcoplasmic reticulum to sequester Ca^{2+} and thereby expedite ventricular active relaxation. Both phospholamban (which increases the rate of Ca^{2+} uptake by sensitizing sarcoplasmic reticulum ATPase to Ca^{2+} when phosphorylated) and Ca^{2+} -ATPase mRNAs were $\sim 40\%$ of adult levels at birth and gradually increased to approach adult levels by *day 15* of development in the mouse heart (14). In cats, the volume fraction of myofibrils in myocardial fibers significantly increased from neonates, to infants, and then to adults (35). Higher myofibril content may increase ventricular recoil after systole and thereby augment peak E velocity. Thus a maturational enhancement in myocardial active relaxation and ventricular recoil likely contributes to the increase in peak velocity of the early ventricular filling wave that occurs during development in mice.

The late ventricular filling wave (A wave) is generated by atrial contraction, and its amplitude depends primarily on the strength of atrial contraction, the atrioventricular orifice area, and ventricular compliance. Peak A velocity was relatively constant throughout development in the mitral and tricuspid orifices, suggesting that these factors remain in balance from late gestation to adulthood in mice.

The peak E/A ratio is a commonly used index for evaluating ventricular diastolic function, but it is sensitive to heart rate and loading conditions (17, 25, 29). In the transitional circulation from fetus to newborn, there are changes in the cardiovascular system that affect preload and afterload of both ventricles and consequently would be anticipated to affect peak E/A ratios. Changes include decreased pulmonary vascular resistance and increased pulmonary venous return, increased systemic vascular resistance and decreased inferior vena caval blood flow, and closure of the foramen ovale and ductus arteriosus (1). Furthermore, there are more gradual but marked changes in heart rate and in pulmonary and systemic arterial pressures during development. As suggested by human studies, the peak E/total TVI ratio is a sensitive index of ventricular diastolic function that is not affected by heart

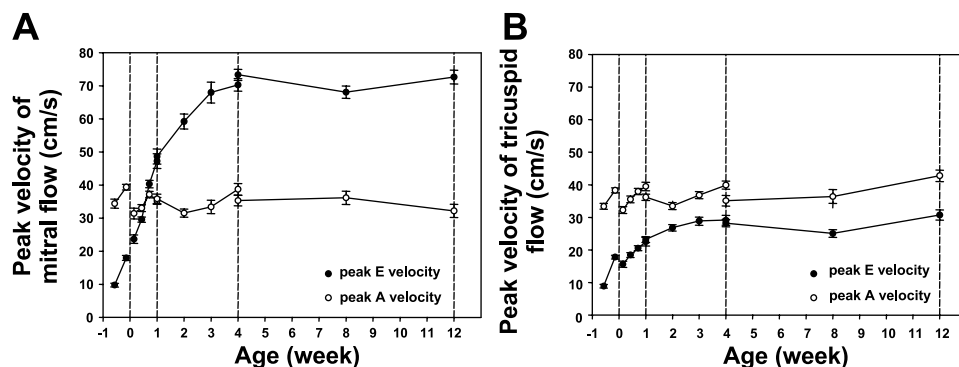


Fig. 6. Peak velocities of E and A waves for mitral flow (A) and tricuspid flow (B) as a function of age (in wk), where zero denotes the time of birth. The peak E and peak A velocities were significantly different ($P < 0.05$) at all time points for both mitral and tricuspid flow spectra except for the mitral flow spectrum on days 3 and 5 after birth. The vertical dashed lines divide data obtained from each of the four age groups.

rate, preload, or afterload (17, 25, 29). In the present study, the peak E/A ratio and peak E/total TVI ratio for both ventricles showed similar changes with age, suggesting that the effect of maturation on ventricular diastolic function dominated effects caused by changes in heart rate and loading conditions during development.

Ventricular IVRT is inversely related to the rate of decline in ventricular pressure during early diastole and therefore depends in part on the rate of myocardial relaxation. Because heart rate increased markedly during development, we expressed the IVRT as a percentage of the R-R interval to make the parameters from different age points comparable and to facilitate comparisons with the human heart. In the present study, left ventricular %IVRT was ~14% in the mouse embryo in late gestation, a value that is similar to prior reports in mouse embryos, in which the ventricles were not differentiated (12–20%) (12, 41). We showed that left ventricular %IVRT decreased with advancing development from 14% at birth to 10% at 4 wk and then remained stable into adulthood in mice. In humans, left ventricular %IVRT is ~16% at 6 wk gestation,

decreases to ~12% in the last trimester of pregnancy, and then stabilizes at 8–9% in children and young adults (13, 22, 42, 44). Thus, at birth, the %IVRT of the heart is greater in mice than humans, again suggesting that the mouse heart is less mature at birth.

Comparison between left and right ventricular diastolic filling patterns. The left and right ventricular diastolic filling patterns, which were similar in the embryo, started to differ within 1 day after birth and continued to gradually diverge to adulthood. As found in our study and previously reported, both ventricles of the embryonic heart at E14.5 are similar in shape and size (19, 21), whereas on the first day after birth, the left ventricle has already started to become morphologically dominant (Fig. 7). The rightward shift of the interventricular septum, caused by the establishment of an interventricular pressure gradient after birth, might be responsible at least in part for the rapid postnatal change in morphological appearance of the two ventricles. Subsequently, structural differences between the ventricles of the newborn mouse heart are enhanced by the differences in the rates of apoptosis and proliferation between the left and right ventricles

Table 3. Comparison of left and right ventricular diastolic flow parameters between male and female adult mice

| | 8 Wk | | 12 Wk | |
|---|-------------|-------------|-------------|-------------|
| | Male | Female | Male | Female |
| Number of mice | 11 | 11 | 11 | 13 |
| Body weight, g | 34.5 ± 0.6 | 26.7 ± 0.5* | 37.7 ± 0.7 | 29.4 ± 0.5* |
| Mitral flow | | | | |
| Heart rate, beats/min | 427 ± 13 | 429 ± 14 | 438 ± 15 | 435 ± 7 |
| Peak E, cm/s | 70.3 ± 2.6 | 65.8 ± 2.6 | 76.0 ± 3.3 | 69.8 ± 2.5 |
| Peak A, cm/s | 39.4 ± 3.1 | 32.9 ± 2.3 | 34.8 ± 3.3 | 30.0 ± 2.4 |
| Peak E/A ratio | 1.93 ± 0.21 | 2.07 ± 0.12 | 2.43 ± 0.26 | 2.46 ± 0.13 |
| Total TVI, cm | 2.5 ± 0.1 | 2.1 ± 0.1* | 2.3 ± 0.1 | 2.0 ± 0.1* |
| Peak E/total TVI ratio, s ⁻¹ | 28.7 ± 1.1 | 31.8 ± 1.4 | 34.3 ± 1.7 | 36.2 ± 1.0 |
| Tricuspid flow | | | | |
| Heart rate, beats/min | 426 ± 15 | 415 ± 10 | 440 ± 18 | 438 ± 10 |
| Peak E, cm/s | 26.1 ± 1.6 | 24.0 ± 1.8 | 30.9 ± 2.3 | 30.6 ± 2.3 |
| Peak A, cm/s | 39.3 ± 2.7 | 33.5 ± 3.1 | 43.7 ± 2.8 | 42.0 ± 2.3 |
| Peak E/A ratio | 0.68 ± 0.03 | 0.73 ± 0.03 | 0.69 ± 0.03 | 0.72 ± 0.04 |
| Total TVI, cm | 1.6 ± 0.1 | 1.4 ± 0.1 | 1.7 ± 0.1 | 1.7 ± 0.1 |
| Peak E/total TVI ratio, s ⁻¹ | 16.4 ± 0.7 | 17.4 ± 0.8 | 17.9 ± 0.9 | 18.7 ± 1.1 |
| Number of mice | 11 | 10 | 11 | 13 |
| LV IVRT, ms | 14.5 ± 0.7 | 13.7 ± 0.9 | 14.3 ± 0.8 | 14.3 ± 0.8 |
| LV %IVRT | 10.2 ± 0.3 | 9.8 ± 0.8 | 10.3 ± 0.5 | 10.2 ± 0.5 |

Values are means ± SE. *Significant difference ($P < 0.05$) compared with the corresponding value of males at the same age.

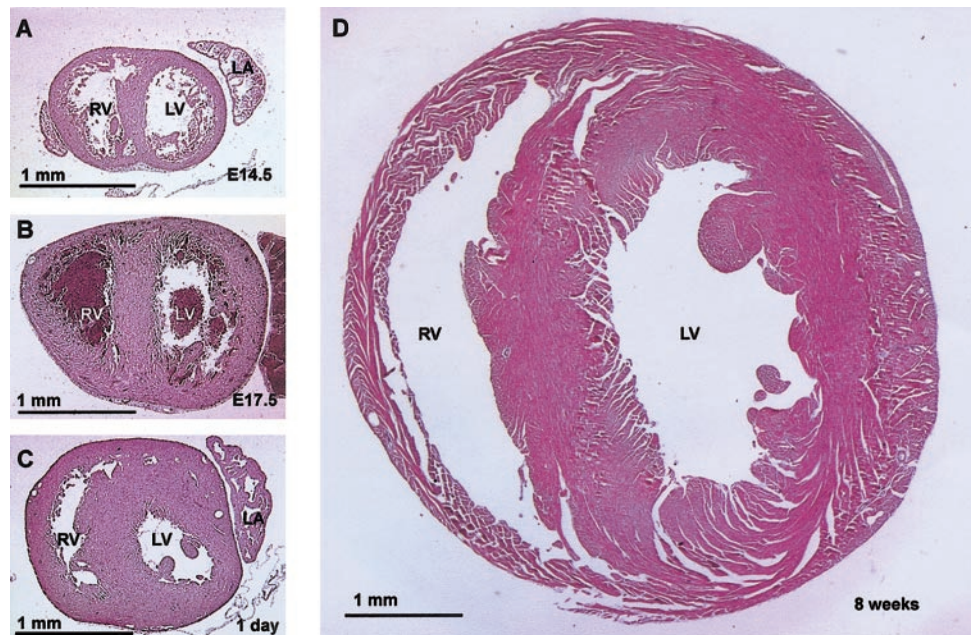


Fig. 7. Histological sections of the ventricles in the short-axis cross section from mouse embryos at E14.5 (A) and at 17.5 days of gestation (E17.5; B), a neonate 1 day after birth (C), and an adult mouse at 8 wk (D).

(8). Structural remodeling presumably plays an important role in the continuing postnatal divergence in the diastolic filling patterns of the two ventricles in mice. However, a similar morphological divergence occurs postnatally in humans; yet, left and right ventricular diastolic filling patterns are similar in human adults, whereas they differ markedly in mice. Thus further study is required to explore the mechanisms responsible for the difference between mice and humans in right ventricular diastolic filling patterns during adulthood.

In the early neonate, similar total TVIs in the mitral and tricuspid orifices (Fig. 4C) suggests that the areas of the mitral and tricuspid orifices were similar, given that stroke volume (which is equal to $\text{TVI} \times \text{orifice area}$) is the same for left and right ventricles after closure of the embryonic shunts. That the tricuspid TVI did not change postnatally suggests that the tricuspid orifice area increased in proportion with the developmental increase in right ventricular stroke volume. However, total TVI of mitral flow increased sig-

nificantly with postnatal development to ~ 3 wk of age (Fig. 4C and Table 2), suggesting a slower rate of growth in mitral orifice area than in left ventricular stroke volume. The difference in TVIs in adult mice suggests that the mitral orifice area is $\sim 65\%$ of that of the tricuspid orifice area. This finding is similar to that of adult humans, in which the mitral orifice area is estimated to be $\sim 70\%$ of that of the tricuspid orifice (46).

Methodological considerations in evaluating ventricular diastolic function. Anesthetic agents have cardiac depressant actions that may introduce confounding factors in hemodynamic assessment. Isoflurane was reported to depress left ventricular systolic and diastolic functions in dogs (30, 31). However, other studies in healthy children (11), dogs (49), and chick embryos (48) found that isoflurane at a low dose did not significantly change ventricular relaxation and myocardial compliance, and isoflurane caused less myocardial depression than other volatile anesthetics. On the other hand, isoflurane may change loading conditions (52)

Table 4. Comparison of ventricular diastolic flow patterns between 1-wk-old mice without anesthesia and the neonatal group at seventh day after birth under anesthesia

| | Mitral Flow | | Tricuspid Flow | |
|----------------------------------|-----------------|------------------|-----------------|------------------|
| | No anesthesia | Anesthesia | No anesthesia | Anesthesia |
| Number of measurements | 8 | 19 | 8 | 19 |
| Body weight, g | 3.5 ± 0.1 | 3.5 ± 0.2 | 3.5 ± 0.1 | 3.5 ± 0.2 |
| Heart rate, beats/min | 423 ± 7 | $388 \pm 10^*$ | 418 ± 13 | 389 ± 10 |
| Peak E, cm/s | 63.1 ± 3.4 | $47.3 \pm 2.2^*$ | 28.7 ± 2.5 | $22.6 \pm 1.3^*$ |
| Peak A, cm/s | 41.0 ± 2.2 | $35.2 \pm 1.0^*$ | 48.6 ± 2.6 | $39.5 \pm 1.3^*$ |
| Peak E/A ratio | 1.55 ± 0.10 | 1.35 ± 0.07 | 0.59 ± 0.03 | 0.56 ± 0.02 |
| Total TVI, cm | 2.1 ± 0.1 | $1.7 \pm 0.1^*$ | 1.8 ± 0.1 | 1.52 ± 0.09 |
| Peak E/total TVI ratio, s^{-1} | 30.4 ± 0.6 | $27.9 \pm 0.7^*$ | 15.8 ± 0.8 | 15.0 ± 0.4 |

Values are means \pm SE; $n = 10$ mice with no anesthesia and 19 mice with anesthesia. In the group without anesthesia, 2 mice were excluded from analysis because of the fusion of E and A waves. *Significant difference ($P < 0.05$) compared with the corresponding value without anesthesia.

Table 5. Comparison of ventricular diastolic flow parameters during anesthesia and at the time of waking up in 2-wk-old mice

| | Mitral flow | | Tricuspid flow | |
|--|-------------------|-------------|-------------------|-------------|
| | During anesthesia | Waking up | During anesthesia | Waking up |
| Number of measurements | 8 | 8 | 10 | 10 |
| Heart rate, beats/min | 406 ± 32 | 416 ± 22 | 417 ± 20 | 410 ± 40 |
| Peak E, cm/s | 60.8 ± 8.9 | 60.4 ± 5.5 | 27.1 ± 3.1 | 25.4 ± 4.2 |
| Peak A, cm/s | 32.1 ± 5.4 | 33.2 ± 4.5 | 36.0 ± 5.0 | 34.6 ± 7.2 |
| Peak E/A ratio | 1.92 ± 0.32 | 1.84 ± 0.15 | 0.75 ± 0.06 | 0.77 ± 0.12 |
| Total TVI, cm | 2.1 ± 0.3 | 1.9 ± 0.3 | 1.6 ± 0.2 | 1.5 ± 0.2 |
| Peak E/total TVI, ratio, s ⁻¹ | 29.1 ± 1.8 | 32.0 ± 3.0* | 17.6 ± 1.3 | 17.5 ± 1.1 |

Values are means ± SE; *n* = 10 mice. In the measurement of mitral flow, 2 mice were excluded from analysis because proper Doppler waveforms could not be obtained at the time of waking up. *Significant difference (*P* < 0.05) compared with the corresponding value during anesthesia.

and consequently affect ventricular filling patterns (28). However, as observed in the present study, the peak E/A ratios for both ventricles in the mice under anesthesia were similar to those of the mice without anesthesia. Velocities were slightly higher in conscious mice, possibly due to the stress of restraint (Table 4). No significant changes were found in most parameters of mitral and tricuspid flows during anesthesia and at the time when the mouse awakened (Table 5). These data suggest that in the present study, isoflurane anesthesia had minimal effect on the diastolic filling pattern of either ventricle.

The heart rate of isoflurane-anesthetized adult mice included in the present study was ~450 beats/min and thus was lower than that of awake, unrestrained adult mice of the same strain (~540 beats/min) obtained by chronic catheterization (6). When the mouse heart rate was higher than ~500 beats/min, we found that the E and A waves often merged, so peak E and peak A velocity could not be measured. The fusion of the E and A waves was relatively more common in adult mice and resulted in the exclusion of ~10% of mice from analysis in this study. On the other hand, exclusion of mice with higher heart rates would tend to reduce the mean heart rate reported for our adult groups. Compared with other commonly used injectable anesthetics, isoflurane had the least effect on the heart rate of ICR mice (52). Also, the anesthetic level

was kept as light as possible in our experiments. Previous studies in normal adult mice report mitral peak E/A ratios from 2.0 to 4.5 (16, 33, 38, 40). Higher peak E/A ratios in some prior reports may be partially explained by lower heart rates (~230–275 beats/min) than in the present study (~450 beats/min) due to differences in anesthetics. Heart rate in embryonic mice from E14.5 to E17.5 in the present study increased from 175 to 230 beats/min and thus was similar to prior reports, where heart rate increased from ~150 to 230 beats/min over a similar age range (12, 41).

In summary, the present study reports the developmental changes in both left and right ventricular diastolic filling patterns from late gestation to adulthood in mice. The mouse body weight continued to increase to ~8 wk, whereas the heart rate increased rapidly from E14.5 to 1 wk after birth, followed by further slight increase to adulthood. On the basis of Doppler diastolic flow parameters, including the peak E/A ratio, peak E/total TVI ratio, and left ventricular %IVRT, the diastolic function of both ventricles improved during late gestation and the early postnatal period and became mature at ~3 wk after birth. The maturation of ventricular diastolic function primarily resulted in an increase in early ventricular filling, likely due to maturation of ventricular recoil and active relaxation mechanisms. Late ventricular filling produced by atrial contraction was relatively constant throughout the study period. Left and right ventricular diastolic filling patterns were similar in embryos with a peak E/A ratio of <1 but diverged markedly during postnatal development, with the mitral peak E/A ratio increasing to >2 but the tricuspid peak E/A ratio remaining <1. Considering the lower peak E/A ratio in the mouse embryo, the later reversal of left ventricular peak E/A ratio in mouse neonates, and the higher %IVRT in mice at birth, mice are born with less mature ventricular diastolic function than humans. As in humans, in mice the growth of the mitral orifice appears to lag that of the tricuspid orifice during postnatal development, and the mitral peak E/A ratio increases during late gestation and postnatal development to reach ~2 in adulthood. However, in the mouse, the tricuspid peak E/A ratio remains <1 into adulthood, in

Table 6. Interobserver and intersession variabilities in the measurement of tricuspid flow parameters in mice

| Parameters | Interobserver Error Within Session | Intersession Error |
|------------------------|------------------------------------|-----------------------|
| Heart rate | 1.3 ± 0.4 (0.2~3.6) | 3.7 ± 1.0 (0.6~9.1) |
| Peak E/A ratio | 6.0 ± 1.7 (2.1~16.8) | 12.6 ± 2.4 (1.6~22.5) |
| Total TVI | 6.8 ± 1.4 (1.6~15.3) | 10.0 ± 1.7 (1.0~19.3) |
| Peak E/total TVI ratio | 3.7 ± 1.3 (0.5~10.9) | 10.5 ± 1.8 (1.6~18.7) |

Values (in %) are means ± SE; *n* = 10 mice (six 6-wk-old female mice and four 8-wk-old male mice). Interobserver error within session and intersession error were calculated as the absolute value of the difference between two measurements divided by the mean of two measurements and as a expressed percentage. Values in parentheses are ranges.

contrast with humans, where it increases postnatally to ultimately become similar to that of the mitral orifice.

The authors thank Dawei Qu for technical assistance, Yong Lu for help with histology, Donald Knapik of VisualSonics for technical support, and the Heart & Stroke Richard Lewar Centre of Excellence of the University of Toronto for lending us the Acuson Sequoia C256.

DISCLOSURES

We thank the Richard Ivey Foundation for funding the purchase of the ultrasound biomicroscope, the Canadian Institutes of Health Research for operating grant support, and the Ontario Research and Development Challenge Fund for fellowship support for Y.-Q. Zhou.

F. S. Foster acknowledges a financial interest in VisualSonics. S. L. Adamson is a member of the Scientific Advisory Board of VisualSonics.

REFERENCES

- Alenick DS, Holzman IR, and Ritter SB. The neonatal transitional circulation: a combined noninvasive assessment. *Echocardiography* 9: 29–37, 1992.
- Chen FC, Yamamura HI, and Roeske WR. Adenylate cyclase and beta adrenergic receptor development in the mouse heart. *J Pharmacol Exp Ther* 222: 7–13, 1982.
- Chien KR. Genes and physiology: molecular physiology in genetically engineered animals. *J Clin Invest* 97: 901–909, 1996.
- Christensen G, Wang Y, and Chien KR. Physiological assessment of complex cardiac phenotypes in genetically engineered mice. *Am J Physiol Heart Circ Physiol* 272: H2513–H2524, 1997.
- De Dios AM, Flores JE, Fischman EA, Martinoli C, Zarlenga B, and Kreutzer EA. [The index of left and right diastolic ventricular filling with 2D Doppler echocardiography in normal children.] *Arch Inst Cardiol Mex* 64: 455–460, 1994.
- Desai KH, Sato R, Schauble E, Barsh GS, Kobilka BK, and Bernstein D. Cardiovascular indexes in the mouse at rest and with exercise: new tools to study models of cardiac disease. *Am J Physiol Heart Circ Physiol* 272: H1053–H1061, 1997.
- Edwards D and Berry JJ. The efficiency of simulation-based multiple comparisons. *Biometrics* 43: 913–928, 1987.
- Fernandez E, Siddiquee Z, and Shohet RV. Apoptosis and proliferation in the neonatal murine heart. *Dev Dyn* 221: 302–310, 2001.
- Foster FS, Pavlin CJ, Harasiewicz KA, Christopher DA, and Turnbull DH. Advances in ultrasound biomicroscopy. *Ultrasound Med Biol* 26: 1–27, 2000.
- Foster FS, Zhang MY, Zhou YQ, Liu G, Mehi J, Cherin E, Harasiewicz KA, Starkoski BG, Zan L, Knapik DA, and Adamson SL. A new ultrasound instrument for in vivo microimaging of mice. *Ultrasound Med Biol* 28: 1165–1172, 2002.
- Gallagher TM, Shields MD, and Black GW. Isoflurane does not reduce aortic peak flow velocity in children. *Br J Anaesth* 58: 1116–1121, 1986.
- Gui YH, Linask KK, Khowsathit P, and Huhta JC. Doppler echocardiography of normal and abnormal embryonic mouse heart. *Pediatr Res* 40: 633–642, 1996.
- Harada K, Tamura M, Toyono M, and Yasuoka K. Effect of dobutamine on a Doppler echocardiographic index of combined systolic and diastolic performance. *Pediatr Cardiol* 23: 613–617, 2002.
- Harrer JM, Haghghi K, Kim HW, Ferguson DG, and Kranias EG. Coordinate regulation of SR Ca²⁺-ATPase and phospholamban expression in developing murine heart. *Am J Physiol Heart Circ Physiol* 272: H57–H66, 1997.
- Hartley CJ, Reddy AK, Madala S, Martin-McNulty B, Vergona R, Sullivan ME, Halks-Miller M, Taffet GE, Michael LH, Entman ML, and Wang YX. Hemodynamic changes in apolipoprotein E-knockout mice. *Am J Physiol Heart Circ Physiol* 279: H2326–H2334, 2000.
- Hoit BD, Khoury SF, Kranias EG, Ball N, and Walsh RA. In vivo echocardiographic detection of enhanced left ventricular function in gene-targeted mice with phospholamban deficiency. *Circ Res* 77: 632–637, 1995.
- Ichihashi K, Ewert P, Welmitz G, and Lange PE. Change in cardiac diastolic function in neonates. *Heart Vessels* 12: 216–220, 1997.
- Iwase M, Nagata K, Izawa H, Yokota M, Kamihara S, Inagaki H, and Saito H. Age-related changes in left and right ventricular filling velocity profiles and their relationship in normal subjects. *Am Heart J* 126: 419–426, 1993.
- Kaufman MH. *The Atlas of Mouse Development*. London: Academic, 1998, p. 177–178 and 230–231.
- Keller BB, MacLennan MJ, Tinney JP, and Yoshigi M. In vivo assessment of embryonic cardiovascular dimensions and function in day-10.5 to -14.5 mouse embryos. *Circ Res* 79: 247–255, 1996.
- Leiva MC, Tolosa JE, Binotto CN, Weiner S, Huppert L, Denis AL, and Huhta JC. Fetal cardiac development and hemodynamics in the first trimester. *Ultrasound Obstet Gynecol* 14: 169–174, 1999.
- Lenihan DJ, Gerson MC, Hoit BD, and Walsh RA. Mechanisms, diagnosis, and treatment of diastolic heart failure. *Am Heart J* 130: 153–166, 1995.
- Linask KK and Huhta JC. Use of Doppler echocardiography to monitor embryonic mouse heart function. In: *Developmental Biology Protocols*, edited by Tuan RS and Lo CW. Totowa, NJ: Humana, 2000, vol. I, p. 245–252.
- Miki S, Murakami T, Iwase T, Tomita T, Nakamura Y, and Kawai C. Doppler echocardiographic transmitral peak early velocity does not directly reflect hemodynamic changes in humans: importance of normalization to mitral stroke volume. *J Am Coll Cardiol* 17: 1507–1516, 1991.
- Nishimura RA, Abel MD, Hatle LK, and Tajik AJ. Assessment of diastolic function of the heart: background and current applications of Doppler echocardiography. Part II. Clinical studies. *Mayo Clin Proc* 64: 181–204, 1989.
- Nishimura RA, Housmans PR, Hatle LK, and Tajik AJ. Assessment of diastolic function of the heart: background and current applications of Doppler echocardiography. Part I. Physiologic and pathophysiologic features. *Mayo Clin Proc* 64: 71–81, 1989.
- Oxorn D, Edelist G, Harrington E, and Tsang S. Echocardiographic assessment of left ventricular filling during isoflurane anaesthesia. *Can J Anaesth* 43: 569–574, 1996.
- Pacileo G, Paladini D, Pisacane C, Palmieri S, Russo MG, and Calabro R. Role of changing loading conditions on atrioventricular flow velocity patterns in normal human fetuses. *Am J Cardiol* 73: 991–993, 1994.
- Pagel PS, Kampine JP, Schmeling WT, and Warltier DC. Alteration of left ventricular diastolic function by desflurane, isoflurane, and halothane in the chronically instrumented dog with autonomic nervous system blockade. *Anesthesiology* 74: 1103–1114, 1991.
- Pagel PS, Kampine JP, Schmeling WT, and Warltier DC. Influence of volatile anesthetics on myocardial contractility in vivo: desflurane versus isoflurane. *Anesthesiology* 74: 900–907, 1991.
- Pedra SR, Smallhorn JF, Ryan G, Chitayat D, Taylor GP, Khan R, Abdolell M, and Hornberger LK. Fetal cardiomyopathies: pathogenic mechanisms, hemodynamic findings, and clinical outcome. *Circulation* 106: 585–591, 2002.
- Pollick C, Hale SL, and Kloner RA. Echocardiographic and cardiac Doppler assessment of mice. *J Am Soc Echocardiogr* 8: 602–610, 1995.
- Reed KL, Sahn DJ, Scagnelli S, Anderson CF, and Shenker L. Doppler echocardiographic studies of diastolic function in the human fetal heart: changes during gestation. *J Am Coll Cardiol* 8: 391–395, 1986.
- Sheridan DJ, Cullen MJ, and Tynan MJ. Postnatal ultrastructural changes in the cat myocardium: a morphometric study. *Cardiovasc Res* 11: 536–540, 1977.
- Sissman NJ. Developmental landmarks in cardiac morphogenesis: comparative chronology. *Am J Cardiol* 25: 141–148, 1970.
- Srinivasan S, Baldwin HS, Aristizabal O, Kwee L, Labow M, Artman M, and Turnbull DH. Noninvasive, in utero imaging of mouse embryonic heart development with 40-MHz echocardiography. *Circulation* 98: 912–918, 1998.

38. **Taffet GE, Hartley CJ, Wen X, Pham T, Michael LH, and Entman ML.** Noninvasive indexes of cardiac systolic and diastolic function in hyperthyroid and senescent mouse. *Am J Physiol Heart Circ Physiol* 270: H2204–H2209, 1996.
39. **Taffet GE, Pham TT, and Hartley CJ.** The age-associated alterations in late diastolic function in mice are improved by caloric restriction. *J Gerontol A Biol Sci Med Sci* 52: B285–B290, 1997.
40. **Tanaka N, Dalton N, Mao L, Rockman HA, Peterson KL, Gottshall KR, Hunter JJ, Chien KR, and Ross J Jr.** Trans-thoracic echocardiography in models of cardiac disease in the mouse. *Circulation* 94: 1109–1117, 1996.
41. **Tobita K, Tinney JP, and Keller BB.** Analysis of murine embryonic cardiovascular phenotype. In: *Cardiovascular Physiology in the Genetically Engineered Mouse*, edited by Hoit BD and Walsh RA. Boston, MA: Kluwer, 2002, p. 353–376.
42. **Tsyvian P, Malkin K, and Wladimiroff JW.** Assessment of fetal left cardiac isovolumic relaxation time in appropriate and small-for-gestational-age fetuses. *Ultrasound Med Biol* 21: 739–743, 1995.
43. **Turnbull DH.** Ultrasound backscatter microscopy of mouse embryos. In: *Developmental Biology Protocols*, edited by Tuan RS and Lo CW. Totowa, NJ: Humana, 2000, vol. I, p. 235–243.
44. **Vaccari M, Crepaz R, Fortini M, Gamberini MR, Scarcia S, Pitscheider W, and Bosi G.** Left ventricular remodeling, systolic function, and diastolic function in young adults with beta-thalassemia intermedia: a Doppler echocardiography study. *Chest* 121: 506–512, 2002.
45. **Verbeke G and Molenberghs G.** *Linear Mixed Models in Practice: A SAS-Oriented Approach*. New York: Springer, 1997.
46. **Westaby S, Karp RB, Blackstone EH, and Bishop SP.** Adult human valve dimensions and their surgical significance. *Am J Cardiol* 53: 552–556, 1984.
47. **Wilson N, Reed K, Allen HD, Marx GR, and Goldberg SJ.** Doppler echocardiographic observations of pulmonary and trans-valvular velocity changes after birth and during the early neonatal period. *Am Heart J* 113: 750–758, 1987.
48. **Wojtczak JA.** The hemodynamic effects of halothane and isoflurane in chick embryo. *Anesth Analg* 90: 1331–1335, 2000.
49. **Yamada T, Takeda J, Koyama K, Sekiguchi H, Fukushima K, and Kawazoe T.** Effects of sevoflurane, isoflurane, enflurane, and halothane on left ventricular diastolic performance in dogs. *J Cardiothorac Vasc Anesth* 8: 618–624, 1994.
50. **Yasuoka K, Harada K, Orino T, and Takada G.** Right ventricular diastolic filling assessed by conventional doppler and tissue Doppler imaging in normal children. *Tohoku J Exp Med* 189: 283–294, 1999.
51. **Zhou YQ, Foster FS, Qu DW, Zhang M, Harasiewicz KA, and Adamson SL.** Applications for multifrequency ultrasound biomicroscopy in mice from implantation to adulthood. *Physiol Genomics* 10: 113–126, 2002.
52. **Zuurbier CJ, Emons VM, and Ince C.** Hemodynamics of anesthetized ventilated mouse models: aspects of anesthetics, fluid support, and strain. *Am J Physiol Heart Circ Physiol* 282: H2099–H2105, 2002.

